ADVANCED FUNCTIONAL MATERIALS

Supporting Information

for *Adv. Funct. Mater.,* DOI: 10.1002/adfm.202105844

Quantum Confinement in Aligned Zigzag “Pseudo-Ribbons” Embedded in Graphene on Ni(100)

Alessandro Sala, Zhiyu Zou, Virginia Carnevali, Mirco Panighel, Francesca Genuzio, Tevfik O. Menteş, Andrea Locatelli, Cinzia Cepek, Maria Peressi,* Giovanni Comelli, and Cristina Africh*

Supporting Information

Quantum confinement in aligned zigzag “pseudo-ribbons" embedded in graphene on Ni(100)

Alessandro Sala, Zhiyu Zou, Virginia Carnevali, Mirco Panighel, Francesca Genuzio, Tevfik O. Menteş, Andrea Locatelli, Cinzia Cepek, Maria Peressi*, Giovanni Comelli, and Cristina Africh*

Table of contents

Figure S1

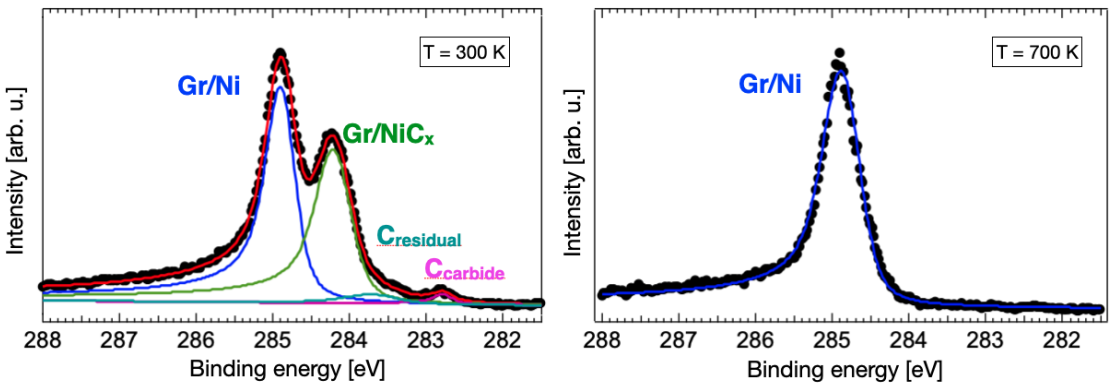

Figure S1 shows μXPS C 1s spectra of graphene grown on Ni(100) measured at room temperature (left) and at 700 K (right). The room-temperature spectrum is fitted using four Doniach-Sunjic peaks following the procedure described in Ref. [18] for the case of Ni(111). From left to right, the components are assigned to the following relevant species: i) graphene strongly interacting with the clean Ni(100) surface (*BE* = 284.9 eV, in blue); ii) non-interacting graphene (*BE* = 284.2 eV, in green); iii) isolated C atoms dissolved into the Ni bulk (*BE* = 283.7 eV, in cyan); iv) surface nickel carbide (*BE* = 282.8 eV, in purple). The latter two components show very low intensity because of the intrinsic low density of C atoms and the small effective photoelectron attenuation length (~ 4.4 Å) at the photon energy used.[S1] By analyzing the components' intensities, considering the attenuation length and the surface densities of C atoms as done in Ref. [18], the surface density ratio between carbide atoms and detached graphene results to be ~ 9%. This is less than half of the expected ratio between surface densities of C atoms for Ni_2C/Ni(100) and graphene, equal to 22%. Such evidence demonstrates that few carbon atoms at the interface are sufficient to break the graphene-substrate interaction for large areas, as in the case of Ni(111).[20] The direct link between nickel carbide and weakly interacting graphene is demonstrated by annealing the sample above the carbon dilution temperature: at 700 K (Figure S1, right), when the carbide carbon atoms have been dissolved in the bulk, the C 1s core level line consists of the strongly

interacting graphene component only (*BE* = 284.9 eV). Such single peak includes the contribution from all the carbon atoms in the 1D moiré; its position, shifted by +0.5 eV with respect to the typical HOPG C 1s line, indicates the overall *n*-doping of graphene on nickel.

[S1] S. Tanuma, C. J. Powell, D. R. Penn, *Surf. Interface Anal.* **2011**, *43*, 689–713

Figure S2

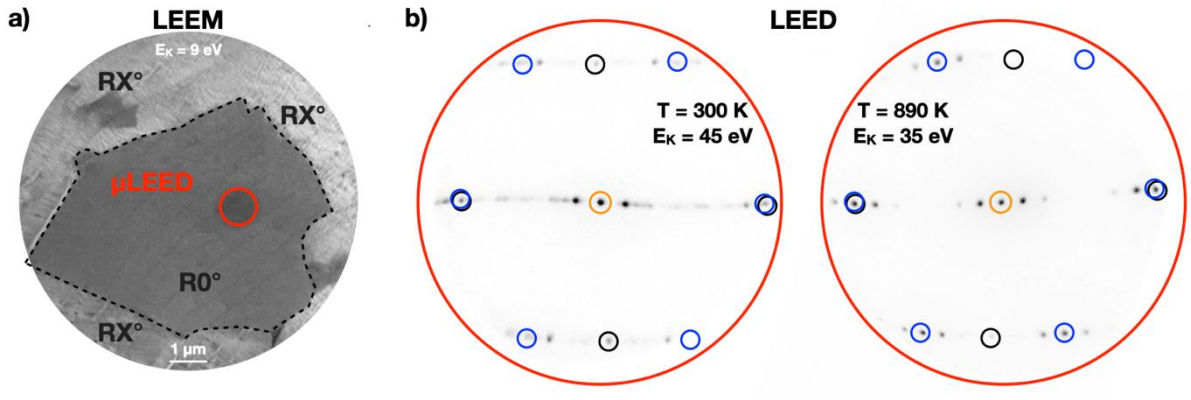

a) LEEM image of one graphene single flake, obtained with electrons backscattered with a kinetic energy of 9 eV. Selected-area LEED (μLEED) was performed by placing a circular aperture of 1 μm to segment the incoming electron beam and illuminate only the area circled in red. b) μLEED patterns (inverted colors) of the single flake collected at room temperature and during annealing at 890 K. The diffraction patterns are slightly distorted by the projection optics of the SPELEEM instrument. The zero-order spot is circled in orange, the first order diffraction spots of graphene are circled in blue, while the Ni(100) ones are circled in black. The presence of GPR at room temperature, whose lateral extent differs from the moiré wiggle, has the effect of blurring the moiré spots along the moiré axis. At high temperature, the dissolution of interfacial carbon atoms into the bulk restores a sharp diffraction pattern. No different LEED patterns were observed by moving the illuminated area across the flake.

Figure S3

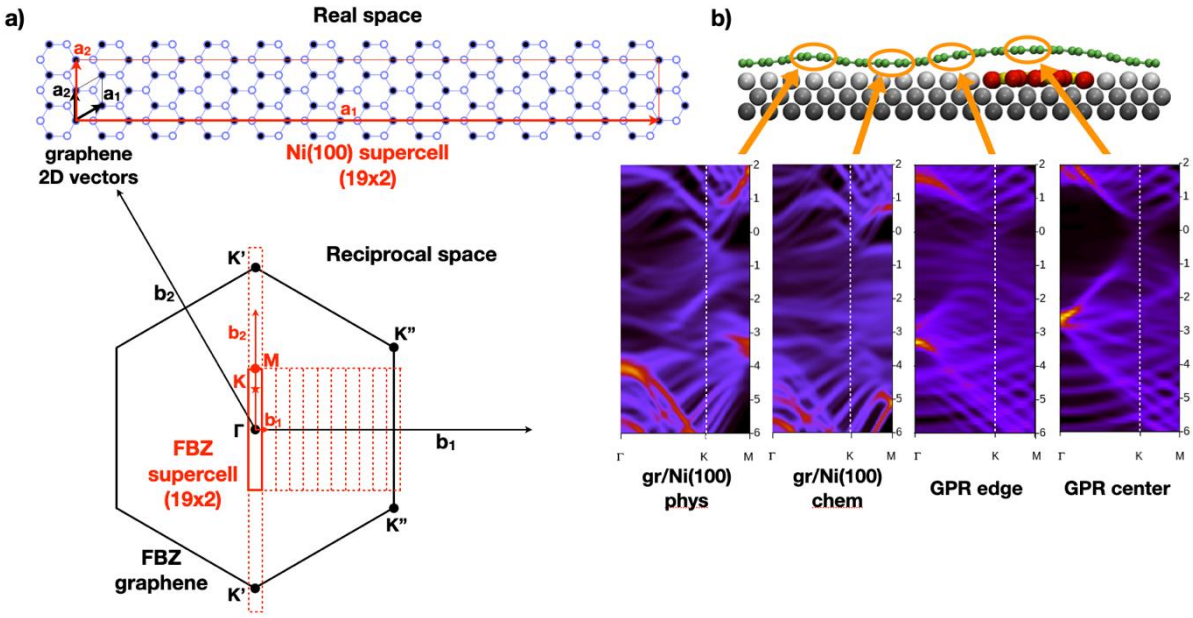

Panel a) shows the lattice structure of the Ni(100) (19x2) supercell (red) in real and reciprocal space, superposed to the unit cell of graphene (black). The supercell is obtained by doubling the vertical size of the Ni(100) (19x1) supercell used to describe the 1D moiré pattern of graphene on Ni(100),[17] in order to accommodate the Ni_2C-(2x2) *clock* reconstruction. Because of the small lattice mismatch, the vector length unit a_0 in the drawing is assumed equal to 2.49 Å and identical for both Ni(100) (square unit cell) and graphene (rhombic unit cell). The supercell, whose multipliers refer to the lattice surface vectors of Ni(100), almost perfectly fits with 11 armchair periods of graphene, which corresponds to $11\sqrt{3}\,a_0 \approx 19.05\,a_0$

The unit cell vectors in real space, $\boldsymbol{a_1}$ and $\boldsymbol{a_2}$, have $\boldsymbol{b_1}$ and $\boldsymbol{b_2}$ as their reciprocal space counterparts, respectively. In the reciprocal space some supercell FBZ are shown (dashed lines) to highlight the folding of graphene high-symmetry points, within a very small tolerance. The six graphene K points fall almost exactly in the same position in the supercell

FBZ. In fact, the horizontal coordinate of K" is not $\frac{(22/19)\pi}{a_0} = 1.158\ \pi/a_0$, as the center of the eleventh Brillouin zone, but $\frac{(2\sqrt{3})\pi}{3a_0} = 1.155\ \pi/a_0$

Panel b) presents the band structures calculated for selected regions of graphene on clean Ni(100), i.e. the ridge and the valley of the wavy 1D moiré pattern, together with the band structure at the edge and at the center of the GPR for comparison. At variance with Figure 1h, the projection here is only on p_z orbitals. The vertical axis displays E-E_F (eV). Despite the blurriness and the superposition of many bands, due to the size of the supercell FBZ, it is evident that graphene in the moiré structure (both in ridge and in valley) on Ni(100) does not show Dirac cones close to the Fermi energy, but exhibits a complex band structure, arising from the strong hybridization between Ni(100) and graphene atoms. Conversely, the GPR shows features reminiscent of the Dirac cone in the center (at E_F, around K point) and of edge states at the borders (flat bands around Γ).

Figure S4

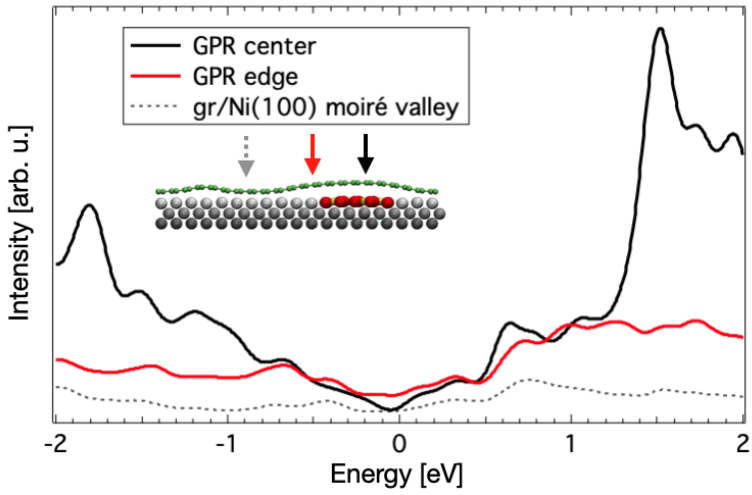

Figure S4 presents the DOS projected along the [100] direction, calculated for three separated regions of the model system (highlighted by arrows over the sketch model in the inlay): the GPR center (in black), the GPR side (in red) and the valley region of the graphene on bare Ni(100) modulated by the 1D moiré (in dashed grey). The projection volume incorporates four adjacent carbon atoms of the graphene. The curves have been rescaled by a factor e^{-2kd} to mimic the effect of a different virtual tip-sample distance *d*, for better comparison with the *dI/dV* spectra shown in Figure 2. *d* was set to 0.0 Å for the black line, 0.5 Å for the red and 1.5 Å for the dashed grey.

Figure S5

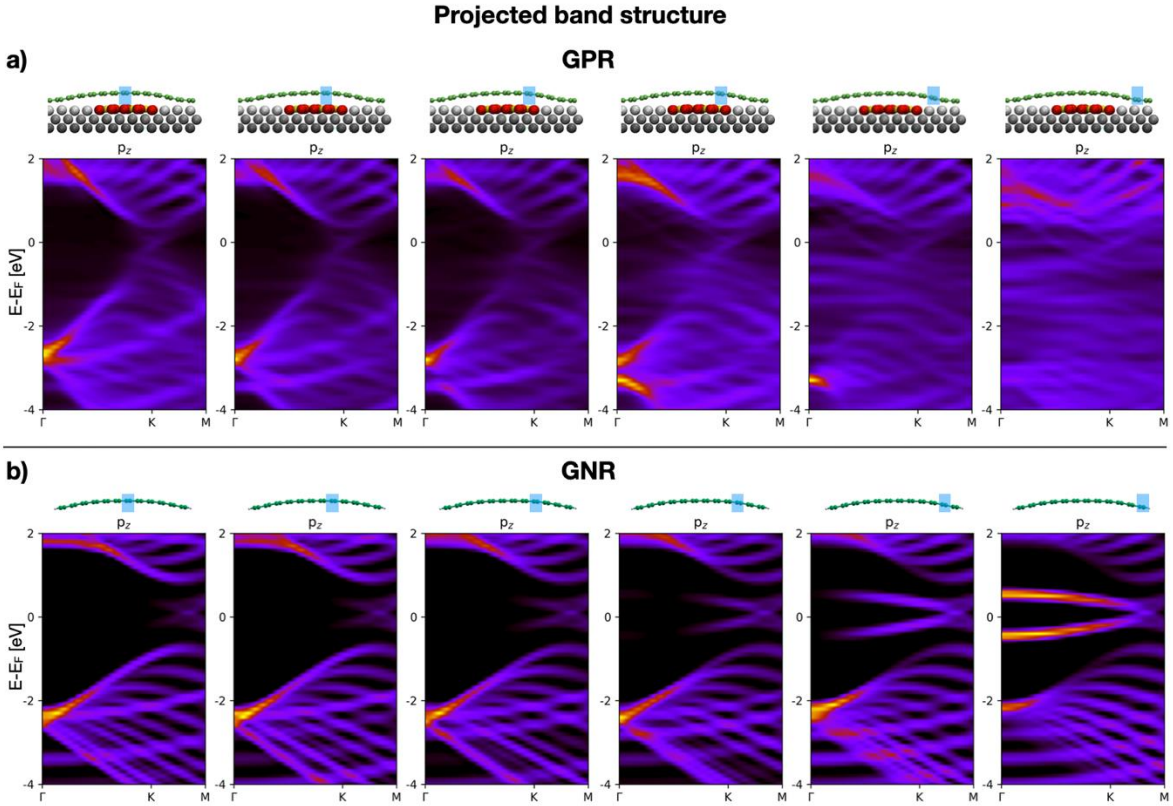

Panel a) shows the band structure of the GPR projected over a single zig-zag row of C atoms, following Ref. [S2], ranging from the center of the ribbon to the edge. The projections are on p_z orbitals. On top of the band structure the model of the GPR is depicted and the atoms involved in the projection are highlighted. Panel b) presents the band structure of an isolated ZZ-GNR with the corresponding projections. The ZZ-GNR is made of C atoms frozen in their GPR positions, with the edges passivated by hydrogen atoms. In both cases, the projection over the outermost C atoms allow the edge states (flat bands) to emerge.

[S2] P. P. Shinde, J. Liu, T. Dienel, O. Gröning, T. Durnslaff, M. Müllinghaus, A. Narita, K. Müllen, C. A. Pignedoli, R. Fasel, P. Ruffieux, D. Passerone, *Carbon* **2021**, *175*, 50-59

Figure S6

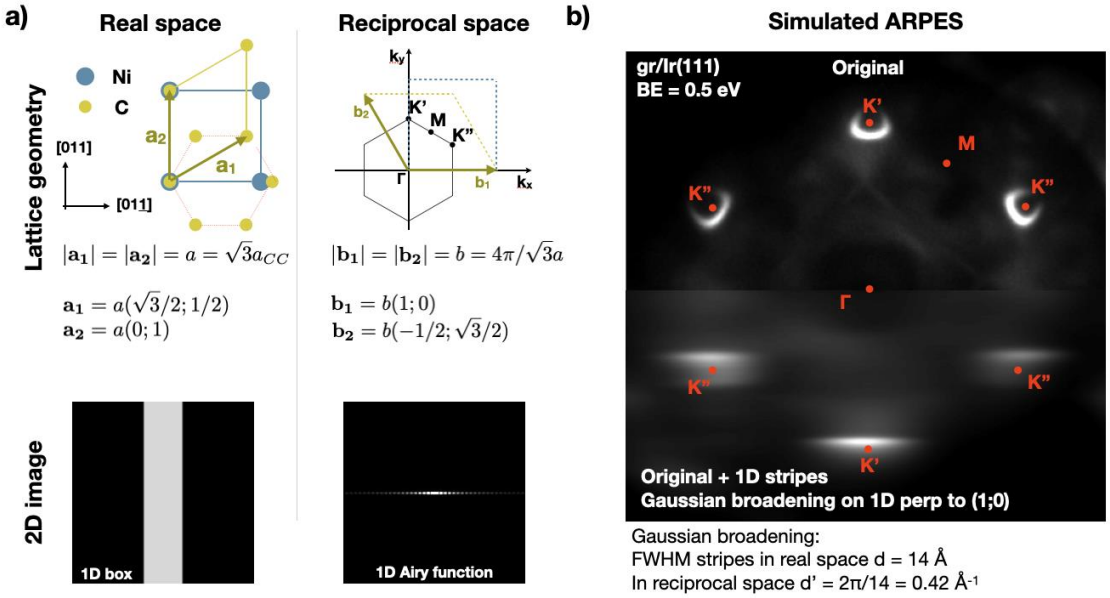

In order to understand the effect of a 1D wavy modulation on the ARPES pattern of a 2D material, one should start from basic considerations on lattice geometry and 2D Fourier transform. In panel a) the lattice geometries of Ni(100) (in cyan) and graphene (in yellow) for both real space and reciprocal space are presented, together with the lattice parameters, as well as the unit cells and the FBZ. With such definition of the axes and of the atomic positions, the 1D modulation develops along the horizontal axis, i.e. the stripes with ZZ edges are placed vertically. Then, in the real space, the GPR can be modeled in first approximation by a single vertical stripe with square profile. The corresponding 2D Fourier transform of such image reveals the frequency map, corresponding to a 1D Airy function along the horizontal direction. Because the GPR height profile is smoother than a sharp box, the central lobe of the 2D Fourier transform becomes very similar to a Gaussian. Therefore, a sequence of aligned 1D vertical structures of smoothed box-like shape in real space are expected to yield Gaussian broadening only on the horizontal direction in reciprocal space. The Full Width Half Maximum (FWHM) of such Gaussian broadening (*d'*) should be the reciprocal of *d*, the FWHM of the 1D structure in real space: $d' = 2\pi/d$.

In order to determine the effect of unidirectional Gaussian broadening on the band structure of the non-interacting 1D GPR, we performed the following simulation. As starting system we considered a graphene single-layer graphene on Ir(111), a non-interacting material, characterized by sharp Dirac cones and almost no doping.[S3] Panel b) displays the ARPES map of the electrons photoemitted by this system with *BE* = 0.5 eV (photon energy 40 eV). The same high symmetry points of the reciprocal space scheme in a) are pinned in red. On the top half the map is shown as measured, on the bottom half an artificial horizontal Gaussian broadening was added, showing its effect on the Dirac cones. The value of the FWHM of the Gaussian broadening was set to mimic the lateral size of the GPR measured with STM. The broadened shape of the Dirac cones remarkably matches the appearance of the π-band of the GPR displayed in Figure 3. It should be noticed that the broadening lifts the 6-fold degeneracy of the Dirac cones, making the K' and K" points inequivalent in the graphene FBZ.

[S3] A. Sala, G. Zamborlini, T. O. Menteş, A. Locatelli, *Small* **2015**, *11*, 5927

Figure S7

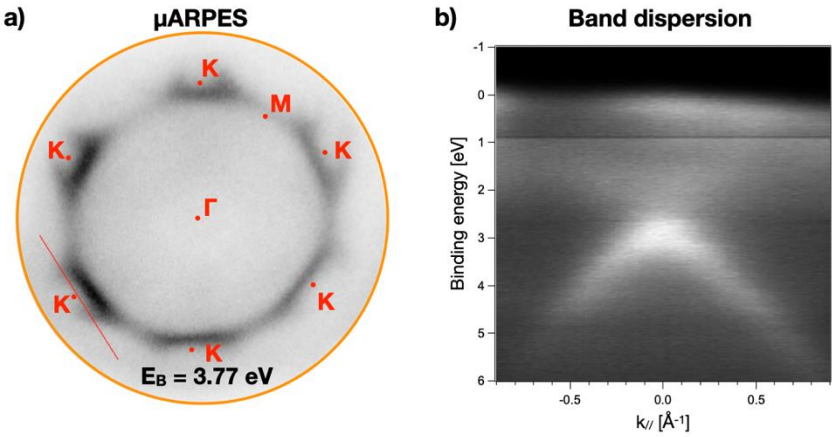

Panel a) shows μARPES map (inverted colors) of the investigated graphene flake, captured from the same illuminated area of Figure 3 but at a sample temperature of 700 K. The photoelectron *BE* is 3.77 eV, the photon energy is 40 eV. Distortions caused by the LEEM/PEEM optics generate achromaticity in the μARPES image; the left side has a smaller BE with respect to the left side.

Panel b) contains the momentum distribution curve of the photoemitted electrons extracted from an intensity line profile (red line in a)) over a stack of μARPES images at different *BE*. Because of the high temperature, the band structure associated to the GPR lifted by the interfacial nickel carbide has disappeared, with only the heavily-hybridized π-band of graphene on clean Ni(100) remaining. The waterfall plot results slightly achromatic due to the distortion of the μARPES.